
KneeHub_DU Calibration Documentation Cleveland State University

Release 0.1

William Zaylor, Ammar Hafez, Jason P. Halloran

Sep 09, 2019

CONTENTS

1	Model Calibration Summary	1
1.1	Knee Model	1
1.2	Optimization Scheme	1
2	Tibiofemoral Model	3
2.1	Ligament Properties	3
2.2	Model Development Deviation	3
3	Experimental Data	5
3.1	Process Experimental Data - DU	5
3.2	Extract Experimental Data	8
4	Optimization Scheme	10
4.1	Test Cases	10
4.2	Control Variables	11
4.3	Control Variable Bounds	13
4.4	Initial Guess	13
4.5	Objective Function	14
4.6	Constraints	14
5	Simulation Steps	16
5.1	Initial Settle Step	16
5.2	Initial Orientation Step	18
5.3	Test Case Step	19
	Bibliography	21

MODEL CALIBRATION SUMMARY

This section summarizes the steps involved in calibrating a finite element knee model. The summary includes links to other chapters where specific details are provided.

These steps apply to the DU data set. The documentation for the OpenKnee(s) data set can be found in a separate document.

1.1 Knee Model

The knee model that was developed during the *Model Development* phase is used for model calibration. Note that a simplified model will be used for calibration, where removal of various anatomy will increase computational efficiency. Details are described in the *Tibiofemoral Model* (page 3) section.

Additionally, a mistake was found in the pACL insertion (specifically the file `dat/DU02/mriData/Segmentation/pAclLine.fcsv`, which is located in the compressed directory titled `DU02ModelDevelopment_IntermediateOutputs.tar.gz`). The mistake likely occurred in 3D Slicer where the insertion point may have been moved when rotating the model in the 3D viewing window. Fortunately, the file is in a local data repository, and original version of the file was restored (before the insertion point was accidentally moved). For the included ligaments, the insertions are the same as are reported in the *Model Development* outputs, except for one of the the pACL tibial insertion points. This is described in the *Model Development Deviation* (page 3) section.

1.2 Optimization Scheme

1.2.1 Optimization Test Cases

There is data for several laxity style test cases available across multiple flexion angles. A subset of these data is used in the calibration procedure. Each objective function evaluation will include 0° and 90° flexion and the following test cases: anterior drawer, posterior drawer, varus moment, valgus moment. The maximum loads from each test case will be included in the objective function, which will result in evaluation of 8 total loading points. See the *Test Cases* (page 10) and *Test Case Step* (page 19) sections for more information.

1.2.2 Control Variables

The knee model is composed of 11 ligament bundles, and the slack length for each bundle is a parameter in the optimization. Specifically, each ligament bundle has two slack length parameters, and these parameters are used to define the slack length of every fiber in the ligament bundle. More details can be found in the *Control Variables* (page 11) section.

Forward Kinematics Model Evaluation

A forward kinematic simulation was used to facilitate definition of the initial guess values as well as bounds for the control variables. The purpose of this simulation is to determine the maximum length of each ligament bundle throughout the experimental data used for calibration. The kinematics from the *calibration test cases* (page 10) are used as inputs to a kinematically driven finite element model, and the lengths of the fibers at the margins of each ligament bundle are recorded. More details can be found in the *Forward Kinematics Simulation* (page 13) section.

Control Variable Bounds

Upper and lower bounds for each control variable are used in the optimization. The lower bounds are set to prevent the optimization algorithm from evaluating slack lengths that may cause instability in the knee model. The upper bounds are used to limit the size of the parameter space. These bounds are defined using the values recorded from the *forward kinematics model evaluation* (page 13). The upper bound for each control variable is defined as the maximum length of the corresponding ligament fiber in the forward kinematics simulation results. The lower bounds are defined as 60% of the upper bound. More details can be found in the *Control Variable Bounds* (page 13) section.

Initial Guess

Each control variable's initial guess value is defined as 90% of the corresponding variable's upper bound (i.e. the maximum length throughout the kinematically controlled simulation). This approach is uniformly applied to every control variable in an attempt to avoid influencing the optimization solution with a judicious selection of initial guess values. More information can be found in the *Initial Guess* (page 13) section.

Optimization Algorithm

The gradient based “SLSQP” algorithm that is available in the SCIPY optimize toolbox will be utilized. This particular approach allows use of inequality constraints and bounds on the control variables. Details are described in *optimization scheme section* (page 10)

1.2.3 Objective Function

The objective function calculates the weighted sum of squared residual between model and experimentally measured kinematics during the simulated *test cases* (page 10). The objective function will evaluate the residual in anterior-posterior tibial displacement, varus-valgus rotation, and internal-external tibial rotation. More details can be found in the *Objective Function* (page 14) section. Information on the specific steps used in the Abaqus simulation can be found in the *Simulation Steps* (page 16) section.

1.2.4 Optimization Constraints

Inequality constraints are used to enforce that each *controlled ligament fiber* (page 11) experiences at least a nominal force of 0.1 N at one point through the simulated *calibration test cases* (page 10).

The constraints are used to prevent the optimization algorithm from effectively removing control variables from the model. A control variable can be effectively removed by specifying a large slack length where the ligament fibers are slack throughout the entire knee model evaluation. In this case the slack fibers will not influence the objective function, and this can result in the optimization algorithm “forgetting” the ligament when it otherwise should not. More details can be found in the *Constraints* (page 14) section.

TIBIOFEMORAL MODEL

The tibiofemoral model that is used in the *optimization scheme* (page 10) is based on the model that was developed in the *Model Development* phase of this project. This section documents any changes that were made to the original model to facilitate the calibration procedure.

Given the model will likely be evaluated hundreds of times, specific anatomy were removed to increase computational efficiency. The patella is unloaded during the experimental laxity tests. As a result, the patella and the patellar ligaments were removed from the knee model. Additionally, the medial and lateral meniscus and mensical attachments were also removed. It is recognized that removing the meniscus may affect the estimate ligament slack lengths due to its potential to provide joint restraint. For the relatively low magnitudes of loading utilized in this work, it is assumed that minimal restraint is provided by the meniscus. This assumption will be tested during *confirmation of the calibration procedure* (page 10) and updated if necessary.

The following sections offer more detail on the model that is used in the *optimization scheme* (page 10), though do note that an error was discovered since the *Model Development* package was disseminated (outlined below). Also note that unlike the Open Knees data, all registration was performed during the *Model Development* phase and has not been reproduced here.

2.1 Ligament Properties

Each ligament bundle's material properties include two slack length values, toe region percent, and stiffness. The calibration procedure will target bundle-specific *slack lengths* (page 11). The toe region percent and the stiffness values are not included in the calibration procedure and will be set to values defined during *Model Development*. In short, ligament stiffness values are defined based on literature values and all toe regions are be set at 6% strain.

2.2 Model Development Deviation

A mistake was found in the pLACL insertion (specifically the file `dat/DU02/mriData/Segmentation/pLACLLine.fcsv` which is located in the compressed directory titled `DU02ModelDevelopment_IntermediateOutputs.tar.gz`). The mistake likely occurred in 3D Slicer where the insertion point may have been moved when rotating the model in the 3D viewing window. This mistake is reflected in the *Model Development* package.

Fortunately the file is in a local repository, and the original version of the file was restored. [Fig. 2.1](#) shows a comparison of pLACL insertion point that was mistakenly moved and reported in the *Model Development* package, and the restored insertion point that is used in the model for calibration.

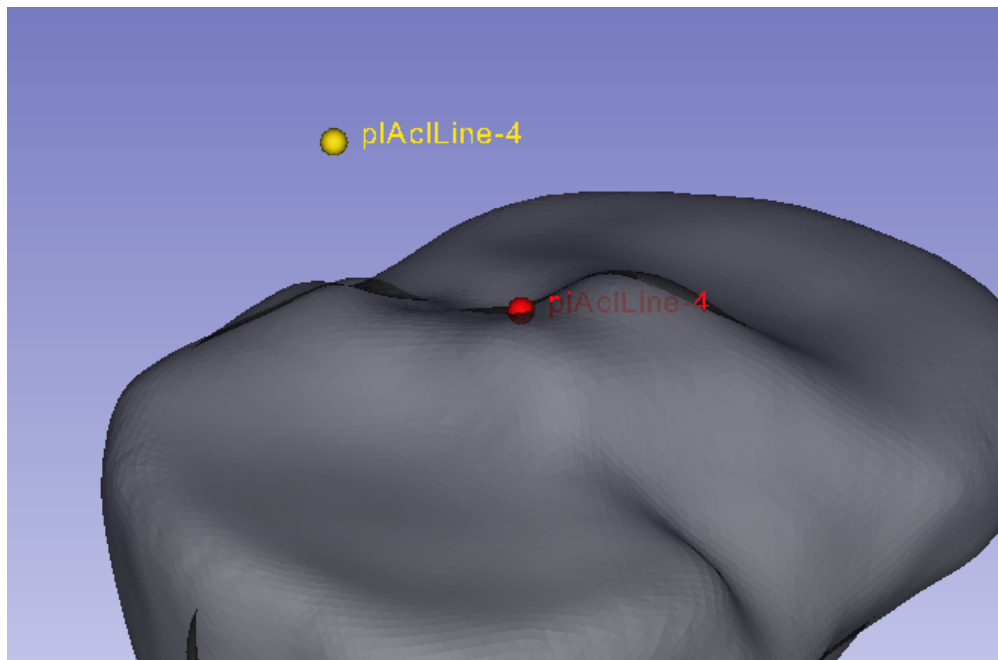


Fig. 2.1: A medial view of the right knee model showing (yellow) the plACL insertion point that was mistakenly moved, and is reported in the *Model Development* intermediate outputs, and is reflected in the plACL mesh. (red) The plACL insertion point before it was mistakenly moved. The red point shows the location of the plACL insertion point that is used in model calibration.

EXPERIMENTAL DATA

Placeholder

3.1 Process Experimental Data - DU

There are two general adjustments that are made to the experimentally measured joint kinematics and kinetics:

- 1) *Time synchronization* (page 5), synchronize the kinematics and kinetics.
- 2) *CSU sign convention* (page 6), convert descriptions of kinematics and kinetics to those used by the CSU lab.

These adjustments can be applied in any order, but for completeness, the data will first be *time-synchronized* (page 5), then the signs of the experimental data will be converted to the *convention used by the CSU lab* (page 6).

3.1.1 Time Synchronization

During a KneeHub meeting on April 2, 2019, a member of the DU lab (Donald Hume) mentioned that there is a potential issue in the synchronization between the experimental loads and displacements. This is an excerpt from that meeting's minutes (found here: <https://simtk.org/plugins/moinmoin/kneehub/2019-04-02>)

... Don and Kevin discussed checking the data and noticed that load and displacement data may need to be resynchronized. Kevin offered providing a resynchronized data. Ahmet recommended keeping the data as is; list this issue as a data limitation at the wiki page and let everyone deal with it in their own way. In response to a question from Jason, Don noted that plots of load vs displacement indicate obvious trends related to this issue...

This section describes how the load and displacement data was resynchronized. A plot of the applied anterior force and resulting anterior displacement demonstrates the time synchronization issue (Fig. 3.1).

A semi-automatic procedure is used to find corresponding points in the experimentally measured load and kinematics curves. Different experimental data files are given for different laxity tests, and each file will be time-synchronized separately. The semi-automatic procedure plots the results from laxity test's primary loading and kinematic direction (i.e. anterior force and anterior displacement for the anterior-posterior drawer test). The user will select a portion of the load curve that appears to be the peak load for the test (Fig. 3.2), and the corresponding part of the kinematics curve. A *knee finding algorithm* (page 6) is used to determine the index of the "knee" for each curve, and the difference between these indices is used to define the kinematics curve's offset (3.1),

$$offset = k_{load} - k_{kinematics} \quad (3.1)$$

where k_{load} is the index of the knee point in the selected portion of the load curve, and $k_{kinematics}$ is the index of the selected portion of the kinematics curve. At least three different offsets are defined at different parts of the curves, and the average offset is used to adjust the indices in the kinematics data (note that the average offset is rounded to

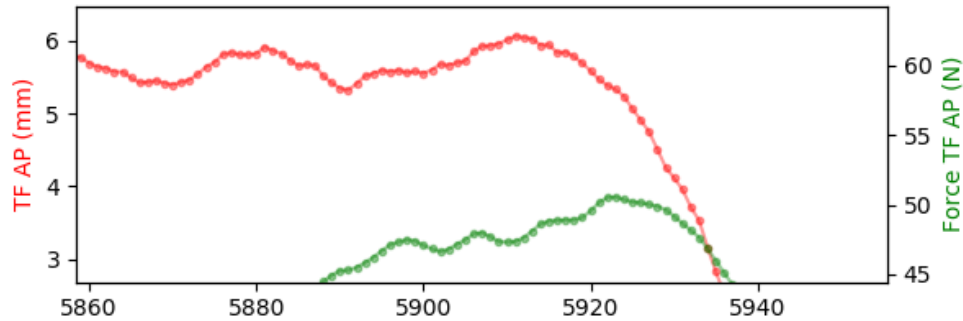


Fig. 3.1: An example of the time synchronization issue. The x-axis is the index in the data point, and the y-axis shows the (green) applied anterior force and the (red) anterior displacement.

an integer if needed). The offset is used to define the number of rows of kinematic data that are removed from the beginning of the .csv files.

Time Synchronization - “Knee” Finding Algorithm

To avoid user variability, a “knee” finding algorithm is used to determine the knee point in a given curve. These knee points are used to find the kinematics that correspond with the applied joint loads. The algorithm that is used is from this website: https://dataplatfrom.cloud.ibm.com/analytics/notebooks/54d79c2a-f155-40ec-93ec-ed05b58afa39/view?access_token=6d8ec910cf2a1b3901c721fcb94638563cd646fe14400fecbb76cea6aaae2fb1

3.1.2 Kinematics and Kinetics Adjustment - CSU convention

The joint kinematics and kinetics are converted to the convention used by CSU. This adjustment is made to keep the experiment

- Medial tibial translation
- Anterior tibial translation
- Superior tibial translation
- Flexion
- Varus
- Internal tibial rotation.

To convert to the CSU convention, the sign of the kinematics for three motions are changed (Table 3.1):

- 1) TF ML (mm) kinematics are multiplied by -1 to convert to medial tibial translation.
- 2) TF VV (deg) kinematics are multiplied by -1 to convert to varus rotation.
- 3) TF IE (deg) kinematics are multiplied by -1 to convert to internal tibial rotation.

To convert to the CSU convention, the sign of the kinetics for three loads are changed (Table 3.1):

- 1) Force TF ML (N) kinetics are multiplied by -1 to convert to medial tibial drawer force.
- 2) Torque TF VV (Nmm) kinetics are multiplied by -1 to convert to varus torque.
- 3) Torque TF IE (Nmm) kinetics are multiplied by -1 to convert to internal tibial rotation torque.

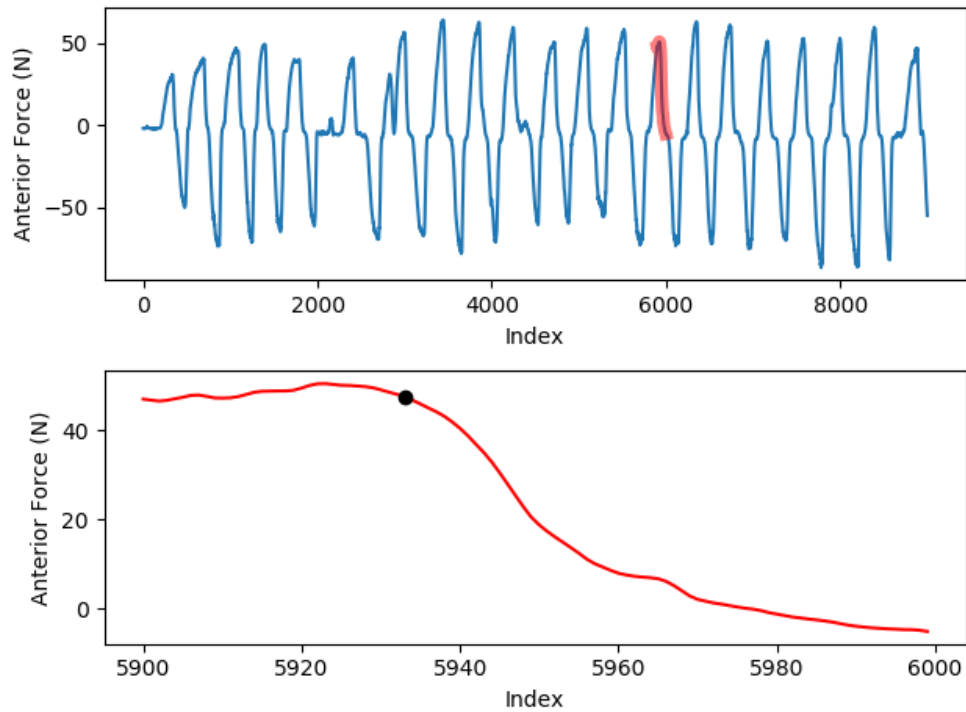


Fig. 3.2: (top) The anterior force during the entire anterior-posterior drawer test, and (red) a portion of the curve that appears to be the peak load for one of the anterior drawer tests. (bottom) The selected portion of the anterior force curve, and (black) the “knee” point of the selected portion of the curve.

Table 3.1: The heading of the reported kinematic and kinetic degrees of freedom, the descriptions of the positive reported values, and the value that is multiplied by the experimental data to convert to the CSU conventions.

Reported	Reported Positive Direction	CSU convention
TF ML (mm)	Lateral tibial translation	-1
TF AP (mm)	Anterior tibial translation	1
TF SI (mm)	Superior tibial translation	1
TF FE (deg)	Flexion	1
TF VV (deg)	Valgus	-1
TF IE (deg)	External tibial rotation	-1
Force TF ML (N)	Lateral tibial drawer force	-1
Force TF AP (N)	Anterior tibial drawer force	1
Force TF SI (N)	Distraction force	1
Torque TF FE (Nmm)	Flexion torque	1
Torque TF VV (Nmm)	Valgus torque	-1
Torque TF IE (Nmm)	External tibial rotation torque	-1

Note: There is no conversion needed for right or left knees because the kinematics and kinetics are measured and applied using the *connector* elements defined in the *Model Development* documentation. These connector elements compose the joint coordinate system ([GS83]), and their definition in developing the model takes into account whether the specimen is a right or left knee.

3.2 Extract Experimental Data

The DU experimentally measured kinematics and kinetics are reported in .csv files. These files contain the experimentally measured tibiofemoral joint loads and the corresponding kinematics. The *time synchronized* (page 5) experimental data is used to parse the different *test cases* (page 10). During preprocessing for model calibration, the indices of the desired points in the experimental test case are defined, and these indices are later used to extract specific kinematics and kinetics from the *time-synced* (page 5) data in the .csv files.

The experimentally measured kinetics and kinematics are used to semi-automatically parse the experimental data. Similar to the *time synchronization methods* (page 5), a custom user interface will plot the experimental kinematics and kinetics curves. The user will select a portion of the load curve that spans the apparent beginning of the test case to the apparent end of the test case (Fig. 3.3). The *knee finding algorithm* (page 6) is used to define the beginning and end of the laxity test (Fig. 3.3). The indices defined by the knee points are used to define beginning and end of the test case. This will be repeated for every *test case* (page 10) that is used in the study.

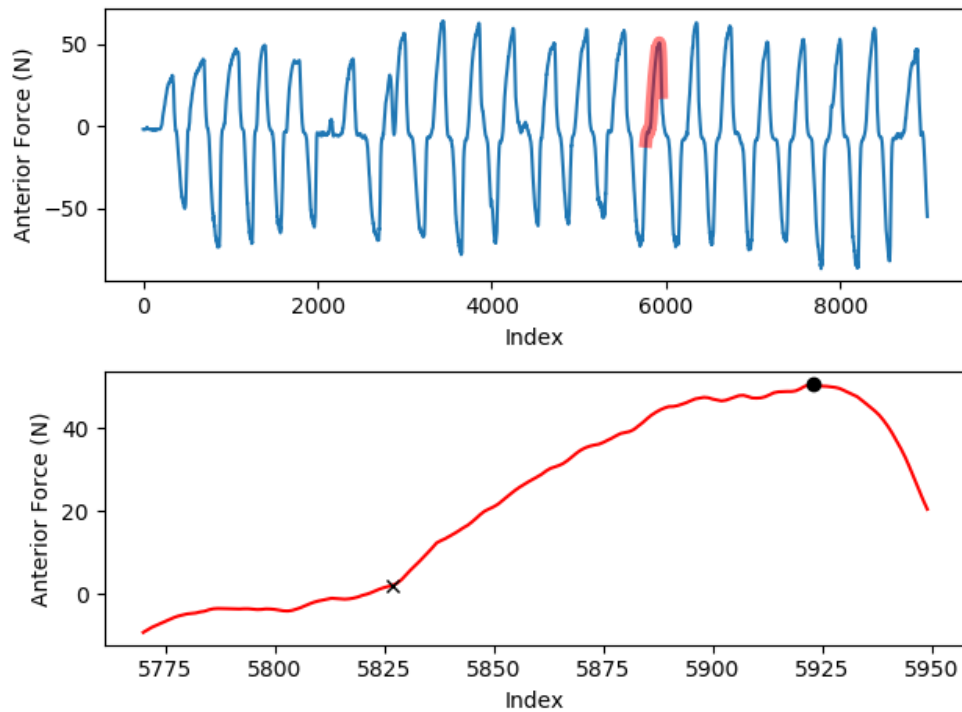


Fig. 3.3: (top) The anterior force during the entire anterior-posterior drawer test, and (red) a portion of the curve that appears to include the start and end of an anterior drawer laxity test. (bottom) The selected portion of the anterior force curve, and (black) the “knee” points of the (x) start and (circle) end of the laxity test. Note that this example does not show the other kinematic or kinetic degrees of freedom that may be used to parse the desired test cases.

OPTIMIZATION SCHEME

A sequential least squares programming (SLSQP) optimization algorithm will be used to calibrate ligament properties. This algorithm was selected because it allows for *inequality constraints* (page 14) and *control variable bounds* (page 13). This algorithm is implemented in the Scipy optimize module.

Initially the convergence tolerance will be set to 1.e-4. It is anticipated this value should be sufficiently small for these analyses, however that will need to be determined at the time of running the calibration procedure. The analyst may observe the solutions have essentially converged, but have not reached the assigned tolerance. To prevent an inordinately long calibration process, the optimization may be terminated prematurely and the lowest objective value used as the calibrated results. If the tolerance value is updated and/or early termination is utilized it will be documented as a deviation.

The SLSQP algorithm is gradient based, and the finite difference method is used to define the gradient. A difference step of -0.1 mm is used in the finite difference calculation. A negative value is used to address cases where a control variable is near a *constraint* (page 14). When a control variable is near a constraint, the corresponding ligament fiber experiences little load during the simulated *test cases* (page 10). Using a negative difference step decreases the ligament fiber's slack length and likely increases that fiber's load during the simulated *test cases* (page 10). This is an attempt to avoid violating *constraints* (page 14) in the finite difference calculation. Note that this finite difference calculation is executed using in-house python code, which allows for direct control of the difference step, and also allows for parallelization of the gradient evaluation.

The following sections offer more details on the parameters used to setup and run the optimization.

4.1 Test Cases

The individual experimental laxity tests that were performed are referred to as a “test case”. Not all of the test cases were used for model calibration. This section describes which test cases were used for model calibration, and which test cases were used to evaluate the results of the model (referred to as “Confirmation” test cases).

4.1.1 Calibration Test Cases

The calibration load cases are the the experimental tests that are simulated as part of the *objective function* (page 14) evaluation. These load cases are a subset of the available data. The *objective function* (page 14) includes the maximum applied loads during the anterior-posterior drawer and varus-valgus tests at 0° and 90° flexion.

4.1.2 Confirmation Test Cases

The experimental test cases that were excluded from the optimization are used to evaluate the estimated ligament properties. These tests include the anterior-posterior drawer and varus-valgus tests at 30° and 60° flexion, and the

internal-external rotation tests at 0°, 30°, 60° and 90° flexion. This evaluation will use the calibrated model to simulate these test cases and measure the error between the calibrated model and experimentally measured kinematics.

Note: Additional test cases and/or test points will be added to the set of calibration test cases if (1) the optimization does not converge or (2) there is excessive error between the calibrated model and experimentally measured kinematics for the calibration and confirmation test cases. Excessive error is defined as kinematic RMS errors that are equal to or greater than 4° for rotations and 4 mm for translations, as would be roughly consistent with recent modeling efforts [EKH+15] and [HCA+16].

4.2 Control Variables

There are two control variables that specify the slack length for each ligament bundle. One control variable specifies the slack length of one margin fiber, and the other specifies the slack length of the other margin fiber (Fig. 4.1). The given slack lengths are used to calculate the strain at the margin fibers of the ligament bundle, and these strains are linearly interpolated to define the slack lengths of the remaining 23 fibers in the ligament bundle.

Note: A ligament bundle’s two given slack lengths are not directly interpolated to assign slack length to the remaining 23 fibers. This is because the femoral and tibial fiber insertion points likely do not lie in the same plane. Additionally, the imaged *insertion-to-insertion length* (page 11) may vary across the ligament bundle due to wrapping.

The given slack lengths for a ligament bundle’s margin fibers, x_0 and x_1 and the fiber’s imaged *insertion-to-insertion length* (page 11), L_0^{im} and L_1^{im} , are used to calculate the strain (ϵ^*) needed to be applied to the fiber’s imaged insertion-to-insertion length to achieve the given slack lengths (x_0, x_1).

$$\epsilon_i^* = \frac{x_i - L_i^{im}}{L_i^{im}} \quad (4.1)$$

Note: ϵ_i^* is the strain that is applied to the ligament relative to the fibers images *insertion-to-insertion length* (page 11). This is not the prestrain carried by the fiber, which is relative to the slack length, $\epsilon = \frac{L^{im} - L^{slack}}{L^{slack}}$

The strains for the two margin fibers ($\epsilon_0^*, \epsilon_1^*$) are linearly interpolated across the ligament bundle. Each fiber’s slack length is calculated using the interpolated strain value and imaged *insertion-to-insertion length* (page 11) (4.1).

4.2.1 Insertion-to-Insertion Length

The insertion-to-insertion length of a ligament fiber is defined as the distance between the fiber’s insertion points, including wrapping around the femur, tibia, meniscus, and cartilage. This length is defined from the results of the “reference simulation” described in Cleveland State University’s *Model Development* documentation.

In short, the ligament geometry was originally defined as springs that spanned between insertion points without any bone, cartilage, or meniscus wrapping. The *reference simulation* enforced ligament wrapping while maintaining the imaged joint position for the ligament insertion points, bones, cartilage, and menisci. After wrapping was enforced, the positions of the ligament nodes were extracted from the *reference simulation* results. These coordinates are used to determine each ligament fiber’s insertion-to-insertion length when the joint is in the imaged position.

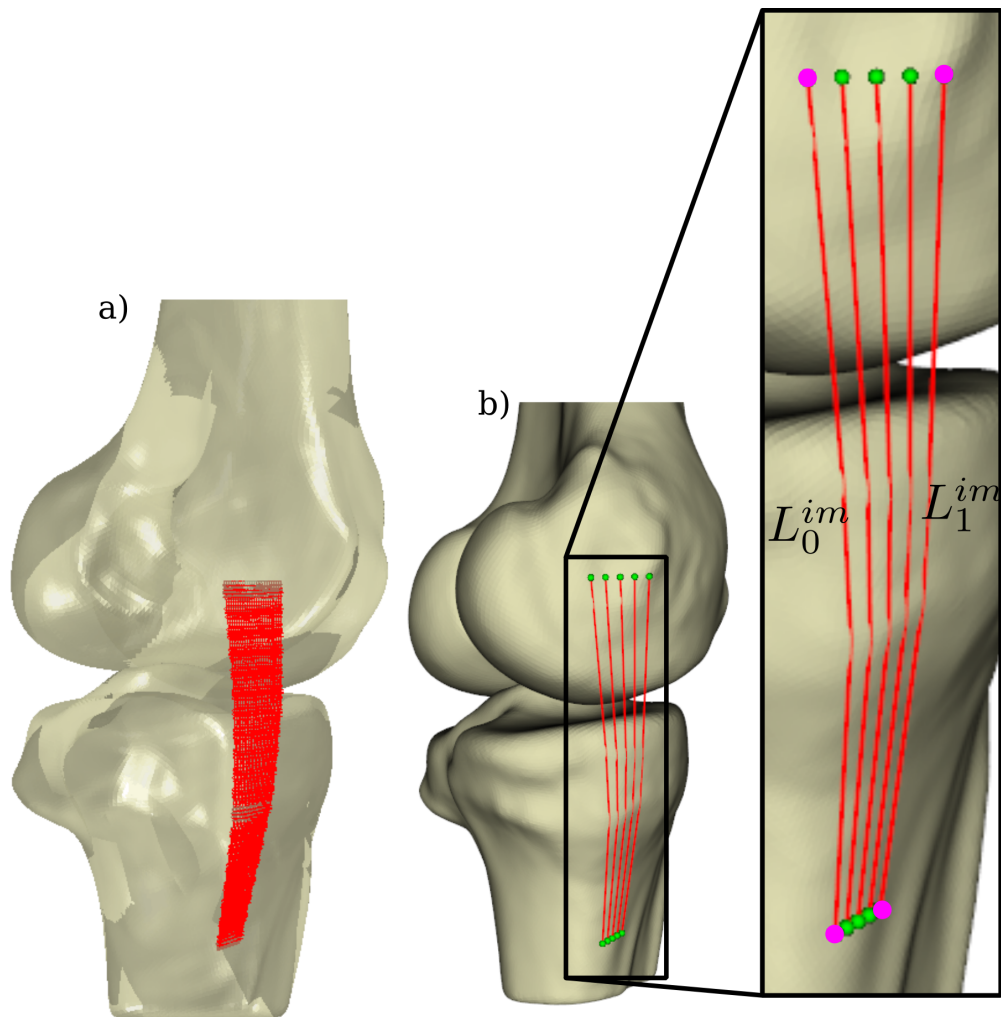


Fig. 4.1: An example of (a) a ligament mesh with 25 fibers from a finite element model. (b) A simplified representation of that same model showing 5 fibers. (inset) The magenta points show the insertions of the fibers at the margins of the ligament bundle insertion, and the insertion-to-insertion length of the first (L_0^{im}) and second (L_1^{im}) fiber at the margins of the insertion in the imaged joint position.

4.3 Control Variable Bounds

In the optimization scheme, upper and lower bounds are specified for the *control variables* (page 11) which define the ligament slack lengths. The bounds serve to avoid unstable simulations and to limit the control variable space. The upper bounds are defined from a rigid body *forward kinematic simulation* (page 13) of the *test cases* (page 10) included in the optimization scheme. The results of this analysis are used to determine the maximum length of the controlled ligament fibers, and these maximum lengths are the upper bounds of the corresponding control variable. The lower bounds are defined as a percentage of the corresponding upper bound.

4.3.1 Forward Kinematics Simulation

A rigid body forward kinematics finite element simulation is used to estimate the insertion-to-insertion length for the ligament fibers for every *test case* (page 10) that is used in the optimization scheme. The forward kinematics simulation utilizes the same tibia, femur and ligament geometries as the model used to calibrate ligament properties. Effectively, it is the same model but setup to run in full kinematics based control. In this simulation, the tibia is fixed and the femur is kinematically controlled in six degrees of freedom. Experimentally measured kinematics for each *test case* (page 10) in the optimization are applied to the femur.

Prestrains are applied to ensure that the ligaments are not slack throughout the simulated test cases. The results of each finite element simulation will be manually inspected to verify each ligament is not slack throughout the simulation. If ligaments are observed to be slack, prestrain for slack ligaments will be decreased until all ligaments are taut.

The results of the forward kinematics simulation are used to determine the ligament fiber lengths that correspond to the *control variables* (page 11). At each of the simulated test points, the node positions of the ligament fibers are used to determine the fiber's insertion-to-insertion length. The maximum insertion-to-insertion fiber length that are achieved in the simulated *test cases* (page 10) are used as the *upper bound* (page 13) for the corresponding *control variable* (page 11).

4.3.2 Upper Bounds

The upper bounds are intended to limit the size of the control variable space. A *forward kinematics* (page 13) is used simulate the *test cases* (page 10) included in the optimization, and the results of these simulations are used to determine the maximum insertion-to-insertion length of the controlled ligament fibers. These maximum insertion-to-insertion lengths are the upper bounds for the corresponding *control variables* (page 11).

4.3.3 Lower Bounds

The lower bounds are intended to prevent the optimization algorithm from evaluating unrealistically small ligament slack lengths. This serves the practical purpose of avoiding unstable simulations caused by extremely tight ligaments. The lower bound for each *control variable* (page 11) is defined as 60% of the corresponding *upper bound* (page 13).

4.4 Initial Guess

The initial guess values for the *slack lengths* (page 11) are defined using the maximum lengths of the ligaments (that was determined when defining the *upper bounds* (page 13) of the optimization variable space). The initial guess for every control variable is the corresponding upper bound (i.e. maximum length) multiplied by 0.9. This value was partially based on experience, and its purpose is to provide an initial guess that satisfies the *inequality constraints* (page 14). This initial guess is uniformly applied to every control variable in an attempt to avoid influencing the optimization solution with a judicious selection of initial guess values.

4.5 Objective Function

For each objective function evaluation, the specified *control variables* (page 11) are applied to the knee model and a subset of the experimental *test cases* (page 10) are simulated. The knee model's joint kinematics [GS83] are measured from the results of the simulation. The objective function is the sum of the squared residual between the model and experimentally measured joint kinematics.

$$f(\bar{x}) = \sum_{j=1}^4 \sum_{k=1}^6 w_k \left(M_{jk}(\bar{x}) - E_{jk} \right)^2 \quad (4.2)$$

$$h(x_i) \geq 0. \text{ for } i = 1 \dots 22$$

where \bar{x} is the set of 22 control variables, x_i is the i^{th} control variable, and $h(x_i)$ is an *inequality constraint* (page 14) that is applied to every control variable, for a total of 22 inequality constraints. The experimental *test case* (page 10) is represented with j , k represents the degree of kinematic freedom, and $w_k = [0, 1, 0, 0, 2, 2]$ is the weight that is applied to each kinematic degree of freedom (Table 4.1).

Table 4.1: The weights and the corresponding kinematic degree of freedom.

i	Weight	DOF
$i = 1$	0	Medial tibial translation
$i = 2$	1	Anterior tibial translation
$i = 3$	0	Superior tibial translation
$i = 4$	0	Flexion
$i = 5$	2	Varus
$i = 6$	2	Internal tibial rotation

The weighting factor, w_k , is used to equate tibial translation to tibial rotations. A weighting factor of 2 was arbitrarily selected to equate 5° of rotational error to 10 mm of anterior tibial translational error.

The weighting factor is also used to exclude kinematic degrees of freedom from the objective function. Flexion is excluded because the experimental flexion angles are prescribed in the finite element model. Medial and superior tibial translation are excluded from the objective function, similar to previous studies [BH96] [BCF+12] [HCA+16]. The same weights are applied to the kinematics, regardless of the experimental test that is being evaluated. This means that the same kinematic degrees of freedom are included in the objective function, regardless of the experimental load case.

4.6 Constraints

Constraints are used in the optimization scheme to enforce that every ligament experiences at least a nominal amount of force at one point the loading cycle (*test cases* (page 10)). These constraints are applied to prevent the optimization algorithm from effectively removing a ligament from the knee model. This can potentially happen if the optimization algorithm assigns an excessively long ligament slack length, preventing that ligament from having an effect on the joint's kinematics, and therefore the *objective function* (page 14).

There is one inequality constraint for every *control variable* (page 11). There is a total of 22 constraints, and each constraint is enforced using the following (4.3).

$$h(x_i) \geq 0$$

$$h(x_i) = (f_i - 0.1)x_i^4 \quad (4.3)$$

where x_i is the control variable, and f_i is the maximum force that the fiber that corresponds to x_i has experienced throughout the simulated *test cases* (page 10). Notice that if f_i is less than 0.1, then $h(x_i) < 0$, and there is a violation of the constraint.

The last term in (4.3) (x_i^4) is used to provide a unique function value for $h(x_i)$. This is necessary because the value f_i can equal zero at multiple values of x_i , and without the last term, $h(x_i)$ can have the same value at multiple values of x_i . The fourth power is used to increase the order of magnitude of the constraint value.

It is also prudent to use the last term in (4.3) (x_i^4) because of the nature of the system. The *control variables* (page 11) are used to define the slack lengths of the ligament fibers. When a constraint is violated, i.e. $h(x_i) < 0$, decreasing x_i will cause $h(x_i)$ to be closer to zero. Given the behavior of the model, decreasing ligament slack lengths can increase the force that the ligament carries in the simulation.

SIMULATION STEPS

This section describes the specific steps and boundary conditions that are used during Abaqus/Explicit FE simulations of the *experimental tests* (page 10). These steps will be executed during every objective function evaluation in the *optimization* (page 10). Laxity tests from two flexion angles are included in the *calibration test cases* (page 10). To limit the simulation time, two separate simulations are run in parallel. One simulation evaluates the *calibration test cases* (page 10) at 0° flexion, and the other simulates the 90° flexion *calibration test cases* (page 10).

Though there are two separate Abaqus simulations, the same steps are applied for each simulation. The differences between the simulations are the magnitude of the specified kinematics and loads in the *Initial Orientation Step* (page 18) and *Test Case Step* (page 19) steps. The magnitude of these loads and boundary conditions are defined as *Amplitudes in the Abaqus .inp files, and the corresponding *processed experimental data* (page 5) is used to define the amplitudes each simulation. This section does not delineate between values that were used for each simulation.

5.1 Initial Settle Step

Before this simulation, the ligament and tendon meshes have been defined from the results of the *reference simulation* during the *Model Development* phase, so there is no overclosure between the ligaments, tendons and other bodies.

The total time for this step is 0.01 seconds.

5.1.1 Interactions

All of the desired interactions are active in this step.

Table 5.1: Active interactions between different bodies and structures during the *Initial Settle* step.

Name	Femur	Tibia	Femoral Cartilage	Medial Tibial Cartilage	Lateral Tibial Cartilage
amACL	x	x	x		
plACL	x	x	x		
aPCL	x	x	x		
pmPCL	x	x	x		
sMCLProx	x	x	x	x	
sMCLDist	x	x	x	x	
dMCL	x	x	x	x	
LCL	x	x			
ALL	x	x	x		x
PFL	x	x	x		x
OPL	x	x	x		x
Femur		x		x	x
Tibia	x		x		
Femoral Cartilage		x		x	x
Medial Tibial Cartilage	x		x		
Lateral Tibial Cartilage	x		x		

5.1.2 Kinematic Boundary Conditions

The rigid bodies are fixed in all degrees of freedom.

Femur

The femur is fixed in all degrees of freedom throughout this step.

Tibia

The tibia is fixed in all degrees of freedom throughout this step.

5.1.3 Kinetic Boundary Conditions

There are no external loads.

Femur

No external loads are applied to the femur in this step.

Tibia

No external loads are applied to the tibia in this step.

5.2 Initial Orientation Step

This step moves the femur from its initial position to the flexion angle for the specific *test case* (page 10). The femur's flexion angle is controlled, but the femur is free to move in other degrees of freedom. The initial flexion angle is defined by the joint's position in the MR images, and the final flexion angle is defined by the flexion angle that is experimentally measured during the first simulated *test case* (page 10). There is a nominal 20 N compressive load applied to the femur throughout this step.

The total time for this step is 0.5 seconds.

5.2.1 Interactions

The orientation of the knee at the end of this step is orientation at the beginning of the first simulated *test case* (page 10). As such, all of the interactions that are desired for the simulated test are active during this step (Table 5.1).

5.2.2 Kinematic Boundary Conditions

Femur

For the simulated test, the femur was unconstrained in all directions except for rotation about the flexion axis. The angle about the femur's flexion axis was assigned throughout this step.

The initial orientation of the knee is known after the femur and tibia coordinate systems are defined with respect to the MR image's coordinate system. The initial flexion angle is used to define the kinematic boundary condition for the femur during this step. Rotation is applied to the connector element that corresponds to the flexion axis (see the *Model Development* documentation for details on the joint coordinate system connectors).

The final flexion angle of the knee is specified as experimentally measured flexion angle at the first simulated *test case* (page 10). Note that this is the absolute flexion angle, which is defined during *experimental data processing* (page 5) and linearly ramped from the reference state. The knee is free to move in all other degrees of freedom.

Tibia

The tibia was fixed in all degrees of freedom.

5.2.3 Kinetic Boundary Conditions

Femur

To reduce the instability in the simulation, a nominal 20 N compressive force is applied to the femur during this step. This force was applied to the connector that defines internal-external tibial rotation axis (see the *Model Development* documentation for details on the joint coordinate system connectors). No other external forces are applied to the femur.

Tibia

No external loads were applied to the tibia in this step.

5.3 Test Case Step

This step applies the experimentally measured loads to the connector elements that define the joint coordinate system ([GS83]). The tibia is fixed throughout this step, the flexion angle is assigned throughout this step, and the femur is free to move in the other five degrees of freedom.

See the *loading profile* (page 19) section for more information on how the *calibration test cases* (page 10) are applied to the knee model in this step.

5.3.1 Interactions

All of the interactions that are assigned for the simulated test are active during this step (Table 5.1).

5.3.2 Kinematic Boundary Conditions

Femur

The femur is unconstrained in all directions except for rotation about the flexion axis. The angle about the femur's flexion axis is assigned using the experimentally measured values throughout this step. The flexion angle is applied using the connector element that defines the joint's flexion axis ([GS83]). See the *Model Development* documentation for more information on how the connector elements are used to define the joint's coordinate system.

Tibia

The tibia is fixed in all degrees of freedom throughout this step.

5.3.3 Kinetic Boundary Conditions

Femur

The *processed experimentally measured joint loads* (page 5) are applied to the appropriate connector elements throughout this step. See the *Model Development* documentation for more information on how the connector elements are used to define the joint's coordinate system.

Tibia

No external loads were applied to the tibia in this step.

Loading Profile

There are a total of eight test cases that are used in model calibration. As described in the *Simulation Steps* (page 16) section, separate simulations at each flexion angle are included in the *calibration test cases* (page 10). Four of these test cases are from the 0° flexion laxity tests, and the other four are from the 90° flexion laxity tests.

A ramp-and-hold scheme is used to apply the desired loads from the *calibration test cases* (page 10) (Fig. 5.1). The loading from each included laxity test is simulated over a step size of 0.5 seconds. The load is linearly increased to the desired value at 0.3 seconds and subsequently held for 0.2 seconds (Fig. 5.1). These loading profiles are used for all 5 degrees of freedom included in the kinetics. Note that the Fig. 5.1 highlights the dominate loading axes and every degree of freedom likely has a non-zero load throughout the simulation. Axis-specific load values will be determined

during extraction of the relevant loading cases using the already developed in house *tool* (page 8) and applied using the connector elements that make up the Grood and Suntay ([GS83]) based connector elements.

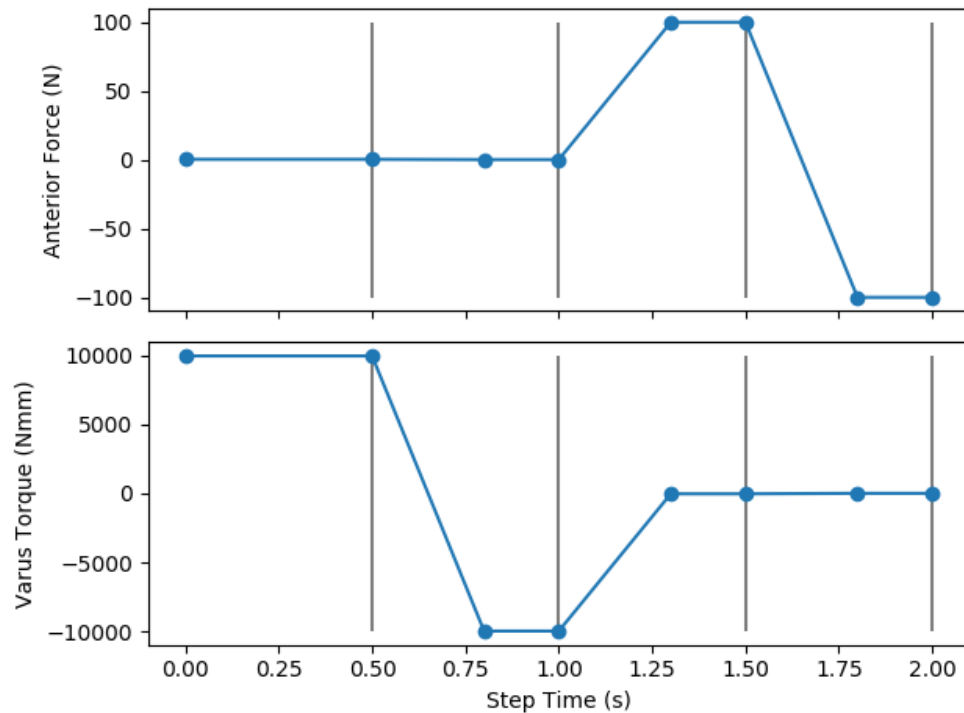


Fig. 5.1: The succession of applied loads will include the varus-valgus torques and anterior-posterior drawer loads throughout a *test case step* (page 19). The vertical lines indicate the points in the step's time where the simulation's results are extracted, which will be used in the *objective function* (page 14). This example shows the applied loads for varus torque, valgus torque, anterior-drawer and posterior drawer tests at 0.5, 1.0, 1.5, and 2.0 seconds, respectively. These points are indicated with the black vertical lines. Note that the values shown in this figure are not the explicit feedback data from OpenKnee(s), but are meant to show the approximate loads along the dominate directions for each test case.

BIBLIOGRAPHY

- [GS83] E. S. Grood and W. J. Suntay. A Joint Coordinate System for the Clinical Description of Three-Dimensional Motions: Application to the Knee. *Journal of Biomechanical Engineering*, 105(2):136–144, May 1983. URL: <http://dx.doi.org/10.1115/1.3138397>, doi:10.1115/1.3138397.
- [EKH+15] Joseph A. Ewing, Michelle K. Kaufman, Erin E. Hutter, Jeffrey F. Granger, Matthew D. Beal, Stephen J. Piazza, and Robert A. Siston. Estimating patient-specific soft-tissue properties in a TKA knee. *Journal of Orthopaedic Research*, pages n/a–n/a, September 2015. URL: <http://onlinelibrary.wiley.com/doi/10.1002/jor.23032/abstract>, doi:10.1002/jor.23032.
- [HCA+16] Michael D. Harris, Adam J. Cyr, Azhar A. Ali, Clare K. Fitzpatrick, Paul J. Rullkoetter, Lorin P. Maletsky, and Kevin B. Shelburne. A Combined Experimental and Computational Approach to Subject-Specific Analysis of Knee Joint Laxity. *Journal of Biomechanical Engineering*, 138(8):081004–081004, June 2016. URL: <http://dx.doi.org/10.1115/1.4033882>, doi:10.1115/1.4033882.
- [BCF+12] Mark A. Baldwin, Chadd W. Clary, Clare K. Fitzpatrick, James S. Deacy, Lorin P. Maletsky, and Paul J. Rullkoetter. Dynamic finite element knee simulation for evaluation of knee replacement mechanics. *Journal of Biomechanics*, 45(3):474–483, February 2012. URL: <http://www.sciencedirect.com/science/article/pii/S0021929011007469>, doi:10.1016/j.jbiomech.2011.11.052.
- [BH96] L. Blankevoort and R. Huiskes. Validation of a three-dimensional model of the knee. *Journal of Biomechanics*, 29(7):955–961, July 1996. URL: <http://www.sciencedirect.com/science/article/pii/0021929095001492>, doi:10.1016/0021-9290(95)00149-2.
- [GS83] E. S. Grood and W. J. Suntay. A Joint Coordinate System for the Clinical Description of Three-Dimensional Motions: Application to the Knee. *Journal of Biomechanical Engineering*, 105(2):136–144, May 1983. URL: <http://dx.doi.org/10.1115/1.3138397>, doi:10.1115/1.3138397.
- [HCA+16] Michael D. Harris, Adam J. Cyr, Azhar A. Ali, Clare K. Fitzpatrick, Paul J. Rullkoetter, Lorin P. Maletsky, and Kevin B. Shelburne. A Combined Experimental and Computational Approach to Subject-Specific Analysis of Knee Joint Laxity. *Journal of Biomechanical Engineering*, 138(8):081004–081004, June 2016. URL: <http://dx.doi.org/10.1115/1.4033882>, doi:10.1115/1.4033882.
- [GS83] E. S. Grood and W. J. Suntay. A Joint Coordinate System for the Clinical Description of Three-Dimensional Motions: Application to the Knee. *Journal of Biomechanical Engineering*, 105(2):136–144, May 1983. URL: <http://dx.doi.org/10.1115/1.3138397>, doi:10.1115/1.3138397.